ADVANCED MATERIALS

Supporting Information

for *Adv. Mater.,* DOI: 10.1002/adma.202102301

Phase–Property Diagrams for Multicomponent Oxide Systems toward Materials Libraries

Leonardo Velasco, Juan S. Castillo, Mohana V. Kante, Jhon J. Olaya, Pascal Friederich, and Horst Hahn*

Supplementary Information

Phase-property diagrams for multicomponent oxide systems towards material libraries

Leonardo Velasco[*]*, Juan S. Castillo, Mohana V. Kante, Jhon J. Olaya, Pascal Friederich, Horst Hahn*

Dr. L. Velasco, J. S. Castillo, M. V. Kante, Prof. Dr. P. Friederich, Prof. Dr. H. Hahn
Institute of Nanotechnology,
Karlsruhe Institute of Technology
Hermann-von-Helmholtz-Platz 1
76344 Eggenstein-Leopoldshafen
Germany
Corresponding author E-mail: leonardo.estrada@kit.edu, leoveles@gmail.com

J. S. Castillo, Dr. J.J. Olaya
Facultad de Ingeniería
Universidad Nacional de Colombia
Av. Cra. 30 # 45-03, Ed. 407
Ciudad Universitaria
Bogotá D.C.
Colombia.

J. S. Castillo, M.V. Kante, Prof. Dr. H. Hahn
Joint Research Laboratory Nanomaterials
Technische Universität Darmstadt
Otto-Berndt-Str. 3,
64206 Darmstadt
Germany.

Prof. Dr. P. Friederich
Institute of Theoretical Informatics
Karlsruhe Institute of Technology
Am Fasanengarten 5
76131 Karlsruhe
Germany

Table of Content

1. Table S1. Chemical composition and crystal structure parameters for the 106 samples.

	Sample	Amount of Liquid [µL] ± 1% dispensing error					Chemical concentration [at. %] ± standard deviation					Crystal structure	Lattice Parameter [Å]	Crystallite size [nm]
		Y	Sm	La	Ce	Pr	Y	Sm	La	Ce	Pr			
SINGLE OXIDES	1	100	-	-	-	-	100	-	-	-	-	Ia-3(100%)	10.57291	139.8
	2	-	100	-	-	-	-	100	-	-	-	Ia-3(100%)	10.89494	159.2
	3	-	-	100	-	-	-	-	100	-	-	P63/m(100%)	a=6.49999, c=3.84036	151.4
	4	-	-	-	100	-	-	-	-	100	-	Fm-3m(100%)	5.38825	150.2
	5	-	-	-	-	100	-	-	-	-	100	Fm-3m(100%)	5.44705	180.4
BINARY OXIDES	6	50	50	-	-	-	49±3	51±3	-	-	-	Ia-3(100%)	10.73466	124.7
	7	-	50	50	-	-	-	51±5	49±5	-	-	Fm-3m(38%), P-3m1(35.6%), P63/m(17.8%), P4/nmm(8.5%)	*5.75345	*104
	8	-	-	50	50	-	-	-	51±3	49±3	-	Fm-3m(95.1%), P321 (4.9%)	*5.51203	*67.5
	9	-	-	-	50	50	-	-	-	52±2	48±2	Fm-3m (100%)	5.39365	109.1
	10	-	-	50	-	50	-	-	53±2	-	47±2	Fm-3m (95.2%), Fm-3m (3.7%)-Y, Fm-3m (1.1%)-Ce	*5.53764	*102.9
	11	50	-	50	-	-	53±3	-	47±3	-	-	Fm-3m (65.1%), P4/nmm(29%), P63/mmc(5.9%)	*10.90395	*125.3
	12	50	-	-	-	50	49±3	-	-	-	51±3	Ia-3(100%)	10.78689	100.6
	13	-	50	-	-	50	-	51±2	-	-	49±2	Ia-3(100%)	10.88347	169.1
	14	-	50	-	50	-	-	50±1	-	50±1	-	Fm-3m (100%)	5.44442	110.5
	15	50	-	-	50	-	53±3	-	-	47±3	-	Fm-3m (100%)	5.36719	101.5
TERNARY OXIDES	16	-	50	50	-	50	-	33±2	35±2	-	32±1	Ia-3(99%), P4/nmm(1%)	*11.01371	*88.4
	17	-	-	50	50	50	-	-	35±2	33±2	32±1	Fm-3m (100%)	5.46875	73.6
	18	50	-	-	50	50	37±2	-	-	32±1	31±1	Fm-3m (100%)	5.38385	88.1
	19	50	50	-	50	-	33±2	33±1	-	34±2	-	Fm-3m(100%)	5.4024	77.5
	20	50	-	50	50	-	34±2	-	34±2	32±2	-	Fm-3m(100%)	5.48594	48.3
	21	50	-	50	-	50	34±3	-	35±3	-	31±1	Fm-3m(100%)	5.51504	81.6
	22	50	50	50	-	-	34±2	32±1	34±2	-	-	Ia-3(41%), P4/nmm(27.4%), P63/m(16.6%), P-3C1(15%)	*10.84606	*86.7
	23	-	50	50	50	-	-	34±2	33±2	33±1	-	Fm-3m (98.9%), P4/nmm(1,1%)	*5.50664	*93.4
	24	-	50	-	50	50	-	35±2	-	34±1	31±1	Ia-3(100%)	10.95435	60.7
	25	50	50	-	-	50	35±2	33±1	-	-	32±2	Ia-3(100%)	10.80213	126.4
QUATERNARY OXIDES	26	50	50	50	-	50	25±5	23±3	26±3	-	26±5	Ia-3(100%)	10.90459	83.2
	27	-	50	50	50	50	-	25±2	26±2	25±1	24±1	Fm-3m(100%)	5.49182	94
	28	50	-	50	50	50	27±1	-	26±1	24±1	23±1	Fm-3m(100%)	5.47679	70.2
	29	50	50	-	50	50	27±1	25±1	-	24±1	24±1	Fm-3m(100%)	5.41069	93.9
	30	50	50	50	50	-	25±2	24±1	27±2	24±1	-	Fm-3m(100%)	5.47701	53.4

Doped with Ce	31	50	50	50	12.5	50	25±3	23±1	24±2	5±1	23±1	Ia-3(100%)	10.95868	82.5
	32	50	50	50	25	50	23±4	23±3	22±3	11±1	21±2	Fm-3m(100%)	5.49655	80.1
	33	50	50	50	37.5	50	20±2	21±2	23±2	15±1	21±1	Fm-3m(100%)	5.48187	71.8
Doped with Y	34	12.5	50	50	50	50	5±1	24±2	24±2	24±1	23±1	Fm-3m(100%)	5.49139	90.9
	35	25	50	50	50	50	10±1	22±1	24±1	23±1	21±1	Fm-3m(100%)	5.48662	86.7
	36	37.5	50	50	50	50	15±2	21±1	23±1	21±1	20±1	Fm-3m(100%)	5.48508	81.9
Doped with Sm	37	50	12.5	50	50	50	25±3	6±1	25±2	23±1	21±1	Fm-3m(100%)	5.47359	73.7
	38	50	25	50	50	50	23±3	10±1	24±3	22±1	21±1	Fm-3m(100%)	5.48112	75.5
	39	50	37.5	50	50	50	22±2	15±1	22±2	21±1	20±1	Fm-3m(100%)	5.47173	77.9
Doped with La	40	50	50	12.5	50	50	26±2	23±1	6±1	23±1	22±1	Fm-3m(100%)	5.43235	89.7
	41	50	50	25	50	50	25±2	21±1	11±1	22±1	21±1	Fm-3m(100%)	5.45701	87.5
	42	50	50	37.5	50	50	21±2	21±1	16±2	21±1	21±1	Fm-3m(100%)	5.45987	84.2
Doped with Pr	43	50	50	50	50	12.5	25±3	23±1	24±3	23±1	5±1	Fm-3m(100%)	5.47296	57.5
	44	50	50	50	50	25	24±2	22±1	23±1	21±1	10±1	Fm-3m(100%)	5.48452	62.1
	45	50	50	50	50	37.5	22±2	21±1	22±2	21±1	14±1	Fm-3m(100%)	5.49842	70.6
Doped with Ce & Y	46	25	50	50	12.5	50	11±2	28±2	29±3	6±1	26±1	Fm-3m(100%)	5.48942	88.7
	47	37.5	50	50	12.5	50	17±2	26±2	26±2	6±1	25±1	Fm-3m(100%)	5.49175	82.1
	48	12.5	50	50	25	50	6±1	27±2	30±3	12±1	25±1	Fm-3m(100%)	5.50687	100
	49	37.5	50	50	25	50	16±1	24±1	25±2	11±1	24±1	Fm-3m(100%)	5.49675	84.9
	50	12.5	50	50	37.5	50	5±1	25±1	28±2	17±1	25±1	Fm-3m(100%)	5.50623	94
	51	25	50	50	37.5	50	12±2	24±1	25±2	17±1	22±1	Fm-3m(100%)	5.48862	85.4
Doped with Sm & Y	52	12.5	25	50	50	50	6±1	13±1	29±2	28±1	24±1	Fm-3m(100%)	5.49107	81.2
	53	12.5	37.5	50	50	50	6±1	17±1	27±2	27±1	23±1	Fm-3m(100%)	5.49239	86.7
	54	25	12.5	50	50	50	13±1	6±1	30±2	27±1	24±1	Fm-3m(100%)	5.48344	73.9
	55	25	37.5	50	50	50	12±2	17±1	25±1	24±1	22±1	Fm-3m(100%)	5.48714	84.5
	56	37.5	12.5	50	50	50	17±2	6±1	29±3	25±1	23±1	Fm-3m(100%)	5.48289	73.2
	57	37.5	25	50	50	50	16±2	12±1	26±2	24±1	22±1	Fm-3m(100%)	5.48685	75.5
Doped with Sm & La	58	50	12.5	25	50	50	30±4	6±1	13±1	27±2	24±2	Fm-3m(100%)	5.44105	80.7
	59	50	12.5	37.5	50	50	26±2	6±1	18±2	26±2	24±1	Fm-3m(100%)	5.46116	74.3
	60	50	25	12.5	50	50	30±2	12±1	6±1	27±1	25±2	Fm-3m(100%)	5.42529	84.1
	61	50	25	37.5	50	50	25±2	12±1	18±2	23±1	22±1	Fm-3m(100%)	5.46363	81.8
	62	50	37.5	12.5	50	50	28±2	17±1	6±1	26±1	23±2	Fm-3m(100%)	5.42862	88.7
	63	50	37.5	25	50	50	23±3	17±1	13±1	24±1	23±1	Fm-3m(100%)	5.43636	76.8
Doped with La & Pr	64	50	50	12.5	50	25	28±2	27±1	7±1	27±1	11±1	Fm-3m(100%)	5.42222	75.3
	65	50	50	12.5	50	37.5	26±2	25±1	7±1	26±1	16±1	Fm-3m(100%)	5.44468	80.2
	66	50	50	25	50	12.5	29±1	26±1	13±1	27±1	5±1	Fm-3m(100%)	5.44681	67.8
	67	50	50	25	50	37.5	24±1	23±1	13±1	24±1	16±1	Fm-3m(100%)	5.44879	74.4
	68	50	50	37.5	50	12.5	26±2	25±1	18±1	26±1	5±1	Fm-3m(100%)	5.46367	67.9
	69	50	50	37.5	50	25	23±2	24±1	18±1	24±1	11±1	Fm-3m(100%)	5.47372	68.9
Doped with Pr & Sm	70	50	25	50	50	12.5	27±2	12±1	29±2	27±1	5±1	Fm-3m(100%)	5.4668	54.1
	71	50	37.5	50	50	12.5	27±2	17±1	26±1	25±1	5±1	Fm-3m(98.3%) - CeO_2, Fm-3m(1.7%) - Ce	*5.46585	*60.5
	72	50	12.5	50	50	25	27±3	6±1	30±3	26±1	11±1	Fm-3m(100%)	5.45911	57.5
	73	50	37.5	50	50	25	26±3	17±1	25±3	22±1	10±1	Fm-3m(100%)	5.47901	60.1
	74	50	12.5	50	50	37.5	27±3	6±1	26±2	25±2	16±1	Fm-3m(100%)	5.47586	64.9

	75	50	25	50	50	37.5	25±2	11±1	25±2	24±1	15±1	Fm-3m(100%)	5.48406	68.6
Doped with Sm & Ce	76	50	12.5	50	25	50	28±1	6±1	28±1	11±1	26±1	Fm-3m(100%)	5.49203	78.7
	77	50	12.5	50	37.5	50	27±2	5±1	27±1	17±1	24±1	Fm-3m(100%)	5.47933	73.5
	78	50	25	50	12.5	50	27±3	12±1	29±3	7±1	25±2	Fm-3m(100%)	5.48839	83.2
	79	50	25	50	37.5	50	24±3	11±1	26±1	16±1	23±1	Fm-3m(100%)	5.49984	77.8
	80	50	37.5	50	12.5	50	27±4	17±1	25±3	6±1	25±2	Fm-3m(100%)	5.499954	85.7
	81	50	37.5	50	25	50	26±1	17±1	24±1	10±1	23±1	Fm-3m(100%)	5.49531	83.2
Doped with Ce & Pr	82	50	50	50	12.5	25	27±3	26±2	30±3	6±1	11±1	Ia-3(100%)	10.94121	67.3
	83	50	50	50	12.5	37.5	27±1	26±2	25±2	6±1	16±1	Fm-3m(100%)	5.48981	76.5
	84	50	50	50	25	12.5	28±1	27±1	28±2	12±1	5±1	Fm-3m(100%)	5.46896	62.8
	85	50	50	50	25	37.5	26±4	22±2	26±3	11±1	15±1	Fm-3m(100%)	5.47508	70.6
	86	50	50	50	37.5	12.5	26±1	26±1	26±1	17±1	5±1	Fm-3m(100%)	5.48653	59.3
	87	50	50	50	37.5	25	24±2	23±2	27±2	16±2	10±1	Fm-3m(100%)	5.48005	66
Doped with Pr & Y	88	25	50	50	50	12.5	12±1	26±2	29±2	27±1	6±1	Fm-3m(98.5%), P4/nmm(1.5%)	*5.49497	*63.6
	89	37.5	50	50	50	12.5	16±2	25±1	28±2	26±1	5±1	Ia-3(100%)	10.95435	60.7
	90	12.5	50	50	50	25	6±1	27±1	28±2	28±2	11±1	Fm-3m(100%)	5.49823	71.5
	91	37.5	50	50	50	25	15±2	23±2	26±3	25±1	11±1	Fm-3m(100%)	5.47675	70.5
	92	12.5	50	50	50	37.5	5±1	24±1	30±2	25±1	16±1	Fm-3m(100%)	5.4952	63.2
	93	25	50	50	50	37.5	11±1	23±1	26±1	24±1	16±1	Fm-3m(100%)	5.49486	77.1
Doped with Y & La	94	12.5	50	25	50	50	6±1	27±1	13±2	28±1	26±1	Fm-3m(100%)	5.46391	105.1
	95	12.5	50	37.5	50	50	7±1	26±2	18±1	25±1	24±1	Fm-3m(100%)	5.46736	90.2
	96	25	50	12.5	50	50	11±1	28±2	7±1	28±1	26±1	Fm-3m(100%)	5.44692	99.1
	97	25	50	37.5	50	50	12±1	23±1	18±1	25±1	22±1	Fm-3m(100%)	5.47179	89.6
	98	37.5	50	12.5	50	50	17±2	25±1	7±1	26±1	25±2	Fm-3m(100%)	5.43249	98.2
	99	37.5	50	25	50	50	17±1	24±1	13±1	24±1	22±1	Fm-3m(100%)	5.45781	83.7
Doped with La & Ce	100	50	50	12.5	25	50	26±3	26±1	7±1	11±1	30±3	Ia-3(100%)	10.85715	101.5
	101	50	50	12.5	37.5	50	26±3	25±2	6±1	18±2	25±2	Fm-3m(100%)	5.42465	93.4
	102	50	50	25	12.5	50	29±2	27±1	13±1	6±1	25±1	Ia-3(100%)	10.89865	98
	103	50	50	25	37.5	50	26±3	24±1	11±1	16±1	23±1	Ia-3(100%)	10.88859	92.5
	104	50	50	37.5	12.5	50	28±3	25±1	17±2	6±1	24±1	Ia-3(100%)	10.93557	87.9
	105	50	50	37.5	25	50	26±1	24±1	17±1	10±1	23±1	Fm-3m(100%)	5.46623	83.3
HEO	106	50	50	50	50	50	19±3	19±1	22±2	21±2	19±1	Fm-3m(100%)	5.46832	76.2

*Crystallite sizes and lattice parameters are given for the major phase.

2. Chemical composition maps

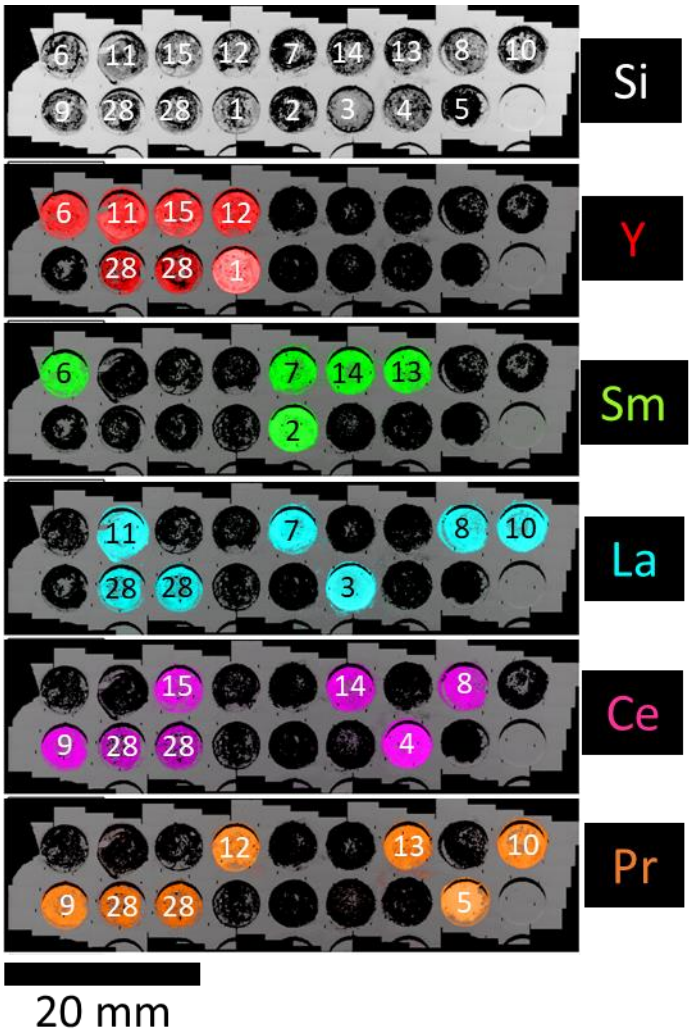

Figure S1. *Chemical composition map obtained from the scanning electron microscope coupled with energy dispersive X-ray spectroscopy (SEM-EDS) for samples 1-15. The distribution of the elements in the quartz plate shows no cross contamination or segregation in the samples. The SEM-EDS map was acquired over an area of 60x14 mm and consist of a total of 106 images. The Si map displays the shape of the wells in the quartz plate. For proof of principle sample 28 was fabricated in the same plate.*

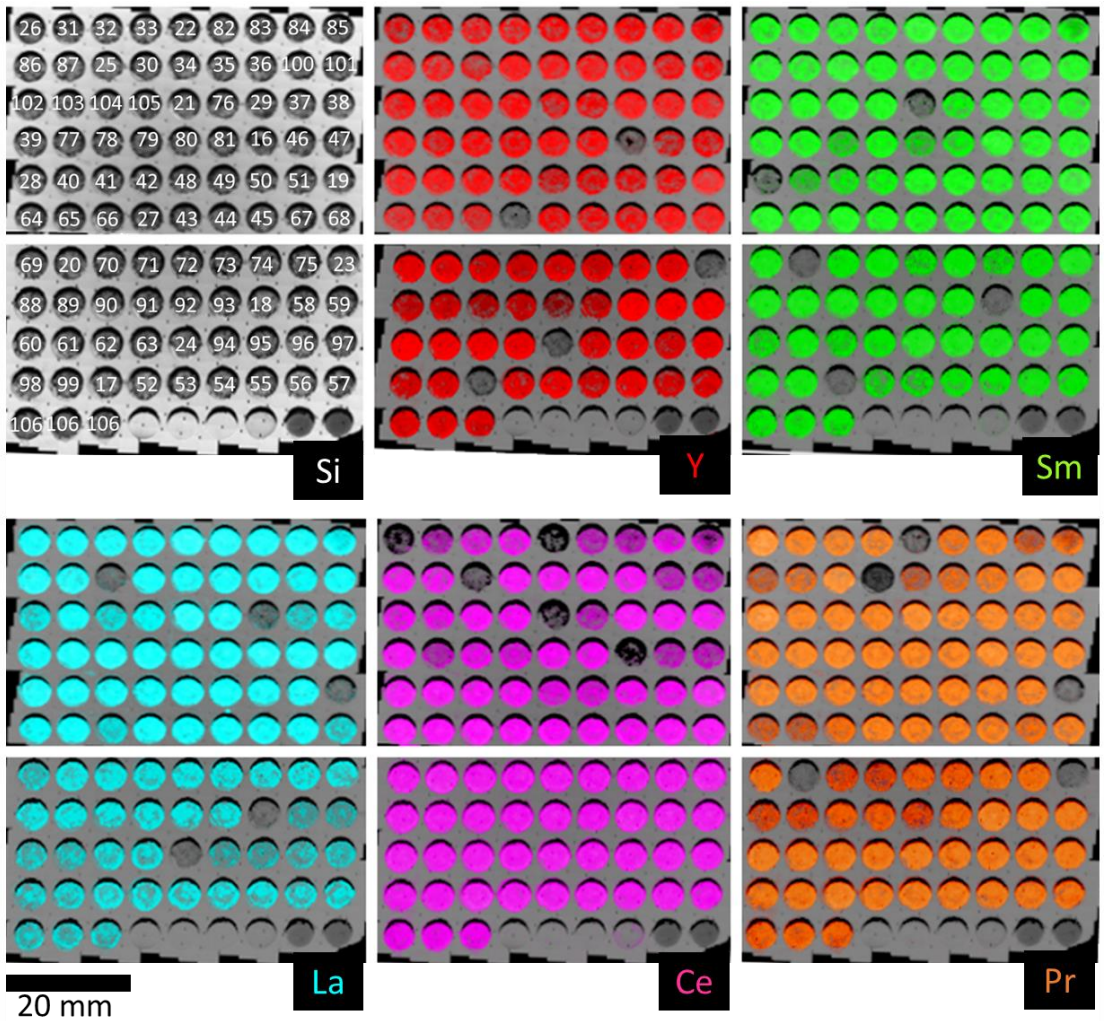

Figure S2. *Chemical composition map obtained from the scanning electron microscope coupled with energy dispersive X-ray spectroscopy (SEM-EDS) for samples 16 - 106. The distribution of the elements in the quartz plate shows no cross contamination or segregation in the samples. The SEM-EDS map was acquired over an area of 60x70 mm and consist of a total of 568 images. The Si map displays the shape of the wells in the quartz plate. Sample 106 was repeated for proof of principle purposes.*

3. X-ray diffractograms for repeated samples without Ce and that displayed a single phase

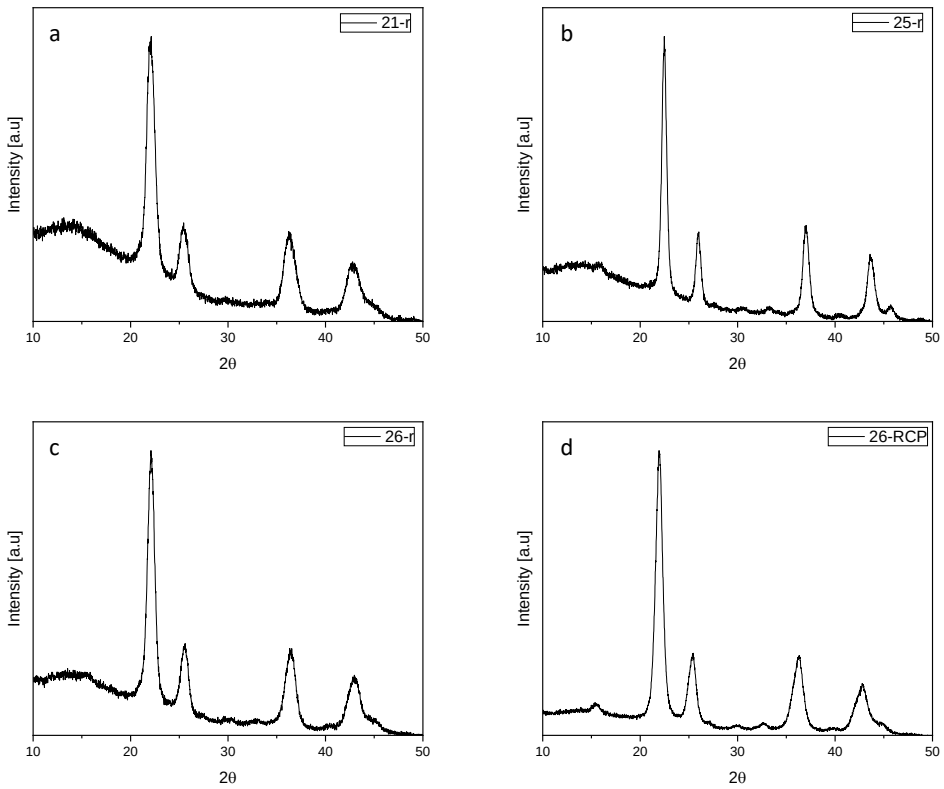

Figure S3. *X-ray difractograms for the repeated samples.* ***a****, sample 21-repeated* $(Y_{0.33}La_{0.33}Pr_{0.33})O_{2-\delta}$ *displays a Fm-3m crystal structure.* ***b****, sample 25-repeated* $(Y_{0.33}Sm_{0.33}Pr_{0.33})O_{2-\delta}$ *displays an Ia-3 crystal structure.* ***c****, sample 26-repeated* $(Y_{0.25}Sm_{0.25}La_{0.25}Pr_{0.25})O_{2-\delta}$ *displays a Fm-3m crystal structure.* ***d****, Sample 26-RCP, prepared by manual reverse coprecipitation following a procedure analogous to the one described by Sarkar et al.,*[1] *displays an Ia-3 crystal structure.*

Sample 26-RCP was prepared by mixing nitrate salts of the corresponding elements (as described in the methodology section of the manuscript for La, Pr, Sm, and Y) in water (50 ml) with a concentration of 0.1 M/L. The precursor solution was titrated into Ammonia solution (28-30% aqueous solution) and the resulting precipitates were separated out using a centrifuge. The precipitates were dried at 80 °C for 12 hours and calcined at 750 °C for 6 hours in an air flowing furnace (heating rate 5 °C/min), and let to cool down to room temperature. The chemical composition of Sample 26-RCP was obtained via SEM-EDS (following the procedure described in the methodology section of the manuscript) and was found to be 25±1 at.% La, 23±1 at.% Pr, 24±1 at.% Sm, and 27±1 at.% Y.

4. Transmission electron microscopy study for the repeated sample 26

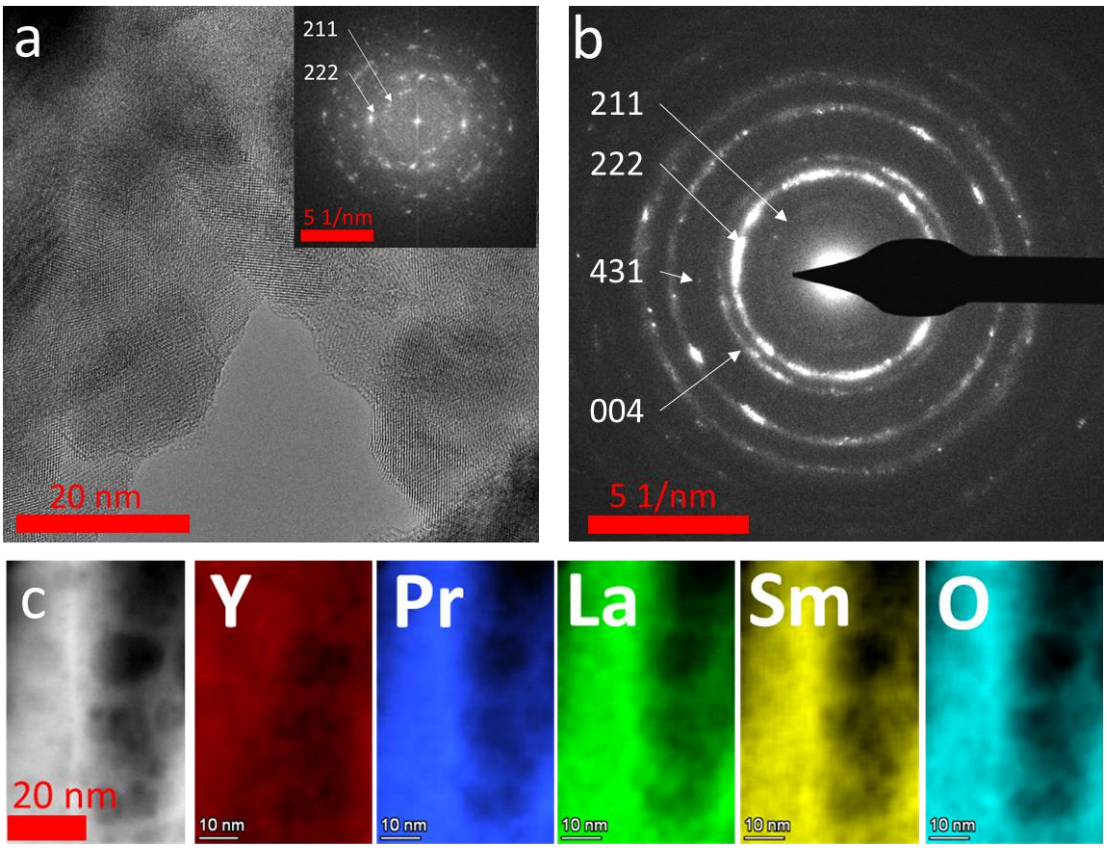

Figure S4. *Repeated Sample 26-r crystal structure and chemical composition characterization conducted by TEM.* ***a****, TEM micrograph showing the crystallinity of the sample.* ***b****, Selected area electron diffraction, the 211 diffraction plane indicates that the sample crystallized in an Ia-3 crystal structure.* ***c****, STEM-EDS chemical composition map demonstrating that the elements are homogeneously distributed. The fast Fourier transform (inset in* ***a****) confirms the Ia-3 crystal structure at nanometer scale.*

5. Machine learning

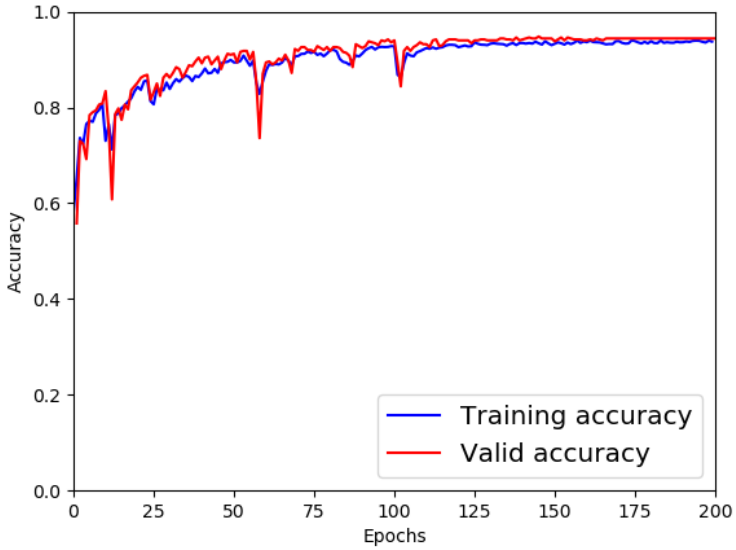

Figure S5. *Training and validation set accuracy as a function of the epochs during training of the convolutional neural network (CNN).*

The CNN was applied to the experimental X-ray diffractograms which were analyzed manually to obtain reference labels for comparison and model evaluation. Even though the entire training set was generated in an artificial way, the performance on the experimental test set was 86 %, with 91 of 106 samples classified correctly. 15 of the pure XRD diffractograms were misclassified as mixed, while all of the mixed XRD diffractograms were detected correctly. Some examples of misclassified diffractograms are shown in the following plots, along with the three reference diffractograms of pure phases, and the SHAP analysis indicating why the neural network (mis)classified the samples as mixed.

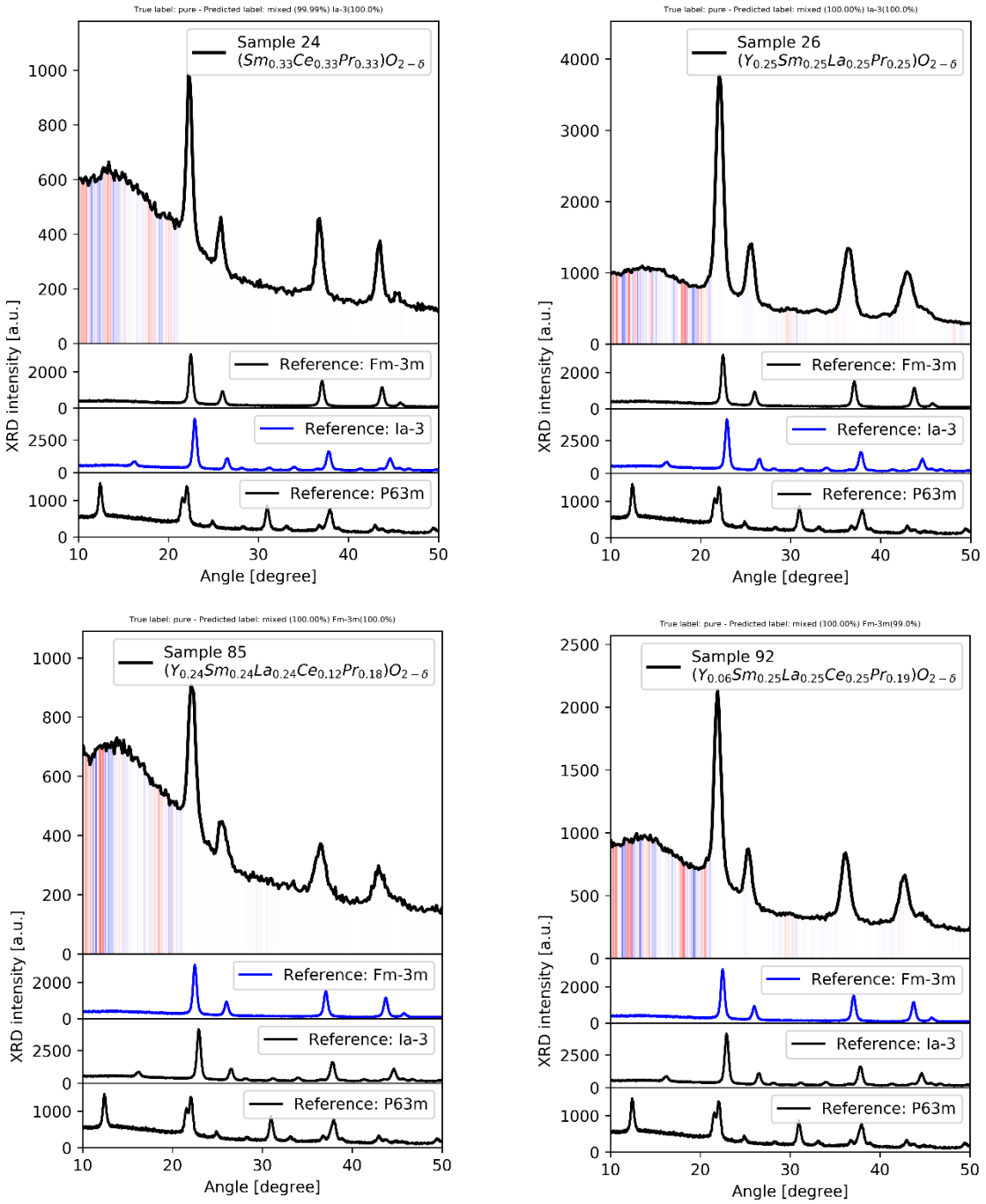

Figure S6. *Samples 24, 26, 85 and 92, manually classified as pure samples, but misclassified by the neural network as a mixed phases. In all cases, the CNN model detects signals in a range of 10-20° and interprets them as signs of mixed phase samples. In samples 26, 85 and 92, the CNN model furthermore finds signals at ~30° and interprets them as traces of an additional phase.*

6. Calculated oxygen vacancy concentration landscape

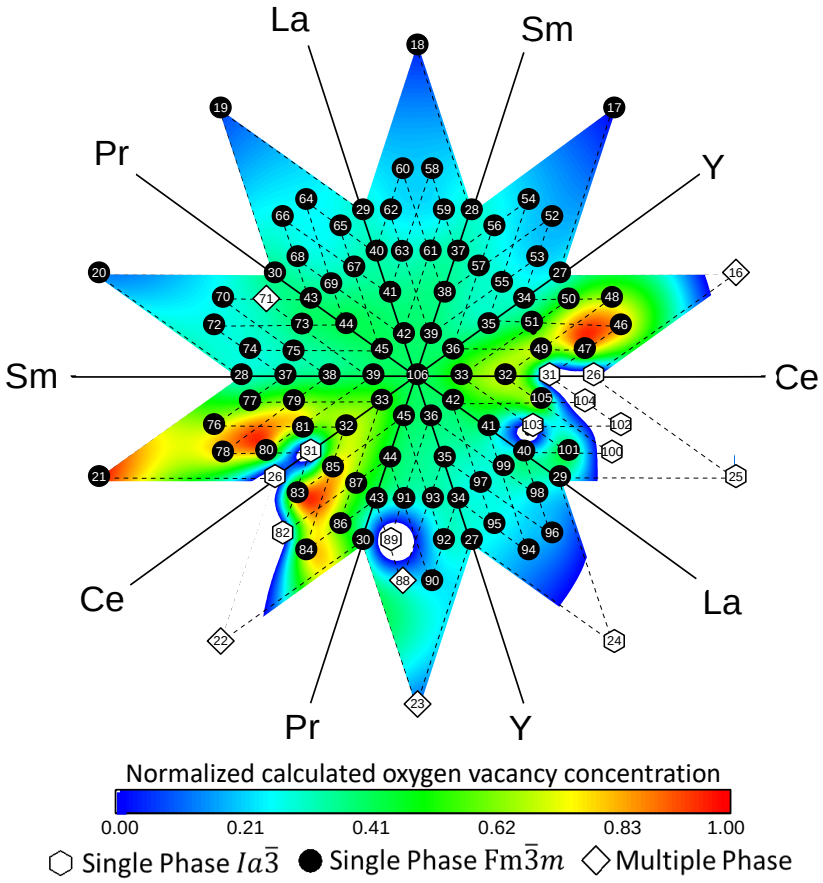

Figure S7. *Landscape for the normalized empirically calculated oxygen vacancy concentration in the multicomponent phase diagram. The symbols are used to highlight if the specific sample has or not multiple phase. Note that in order to fit all the 91 samples in one multicomponent phase diagram the constituent element axes are repeated, and the amount of points in the figure increases by 20. The blank sections in the contour plot belong to samples that have an Ia-3 crystal structure or multiple phase systems.*

Flourite structure is a CaF2 type structure. Each unit cell in a CaF2 structure has 4 cations and 8 anions with a ration of 1:2. Most of the oxides synthesized in this study have a fluorite structure. Therefore, 2 oxygen ions exist for each cation and the cation charge should be $^{+4}$. Oxygen vacancies arise as the charge of the cation deviates from $^{+4}$.

For a Fluorite structure with multiple cations and mix oxidation states (e.g., $^{+3,+4}$), the calculation of the oxygen vacancy concentration can be obtained based on $A_{1-x}^{+4}B_{x}^{+3}O_{2-\frac{x}{2}}^{-2}$, where A is any cation with $^{+4}$ charge state and B is any cation with $^{+3}$ charge state (in the case of Pr we assumed mixed charge state to be 10% of $^{+3}$). The chemical composition in Table S1 was used for the value of x.

7. Polyamide tape X-ray diffractogram

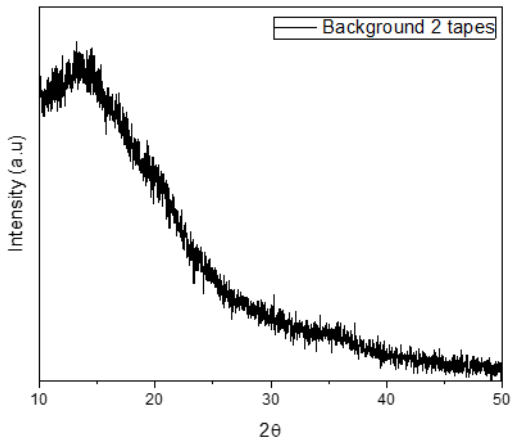

Figure S8. *X-Ray Diffractogram for polyamide tapes.*

8. Table S2. Calculated band gap and comparison with samples reported in literature

Table S2. Calculated band gap for the 106 samples.

	Sample	Chemical concentration [at. %] ± standard deviation					Band gap [eV]	Reported band gap [eV]	Reported oxides in the literature
		Y	Sm	La	Ce	Pr			
SINGLE OXIDES	1	100	-	-	-	-	5.718±0.004	5.72[2,3]	[4,5]
	2	-	100	-	-	-	4.828±0.011	4.9[3]	[5,6]
	3	-	-	100	-	-	5.208±0.01	5.4[3,7]	[5,8]
	4	-	-	-	100	-	3.376±0.003	3.17[3,7]	[9]
	5	-	-	-	-	100	2.468±0.038	3.2[3,10]-2.5-3.9[11]	[12]
BINARY OXIDES	6	49±3	51±3	-	-	-	4.977±0.001	5.97[13]	[14]
	7	-	51±5	49±5	-	-	4.838±0.006		[5]
	8	-	-	51±3	49±3	-	3.234±0.005	3[15]	[16,17]
	9	-	-	-	52±2	48±2	1.864±0.02	2.65 – 2.97[18]	[19,20]
	10	-	-	53±2	-	47±2	1.992±0.015		[21]
	11	53±3	-	47±3	-	-	5.063±0.013	5.5 – 5.7[22]	[23]
	12	49±3	-	-	-	51±3	2.004±0.005		[24]
	13	-	51±2	-	-	49±2	2.013±0.022		
	14	-	50±1	-	50±1	-	3.3±0.011	3.58[25]	[26]
	15	53±3	-	-	47±3	-	3.308±0.007	3.01[27]	[28]
TERNARY OXIDES	16	-	33±2	35±2	-	32±1	2.015±0.012		
	17	-	-	35±2	33±2	32±1	1.843±0.022	1.95[29]	[29,30]
	18	37±2	-	-	32±1	31±1	1.92±0.028	1.95[27]	[31]
	19	33±2	33±1	-	34±2	-	3.29±0.019		
	20	34±2	-	34±2	32±2	-	3.299±0.01	3.22[32]	[33,34]
	21	34±3	-	35±3	-	31±1	2.04±0.044	2.02[35]	
	22	34±2	32±1	34±2	-	-	5.01±0.018		[5]
	23	-	34±2	33±2	33±1	-	3.349±0.015		[26]
	24	-	35±2	-	34±1	31±1	2.059±0.025		
	25	35±2	33±1	-	-	32±2	1.98±0.013		
QUATERNARY OXIDES	26	25±5	23±3	26±3	-	26±5	2.031±0.027		
	27	-	25±2	26±2	25±1	24±1	2.018±0.016	2.14[29]	[29]
	28	27±1	-	26±1	24±1	23±1	1.988±0.033	1.98[29]	[29]
	29	27±1	25±1	-	24±1	24±1	2.052±0.03		
	30	25±2	24±1	27±2	24±1	-	2.251±0.006		
Doped with Ce	31	25±3	23±1	24±2	5±1	23±1	2.123±0.059		
	32	23±4	23±3	22±3	11±1	21±2	2.074±0.036		
	33	20±2	21±2	23±2	15±1	21±1	2.069±0.028		
Doped with Y	34	5±1	24±2	24±2	24±1	23±1	2.029±0.016		
	35	10±1	22±1	24±1	23±1	21±1	2.049±0.006		
	36	15±2	21±1	23±1	21±1	20±1	2.042±0.013		

Doped with Sm	37	25±3	6±1	25±2	23±1	21±1	2.022±0.014
	38	23±3	10±1	24±3	22±1	21±1	2.03±0.005
	39	22±2	15±1	22±2	21±1	20±1	2.055±0.042
Doped with La	40	26±2	23±1	6±1	23±1	22±1	2.032±0.042
	41	25±2	21±1	11±1	22±1	21±1	2.031±0.024
	42	21±2	21±1	16±2	21±1	21±1	2.058±0.017
Doped with Pr	43	25±3	23±1	24±3	23±1	5±1	2.222±0.022
	44	24±2	22±1	23±1	21±1	10±1	2.146±0.026
	45	22±2	21±1	22±2	21±1	14±1	2.093±0.01
Doped with Ce & Y	46	11±2	28±2	29±3	6±1	26±1	2.019±0.044
	47	17±2	26±2	26±2	6±1	25±1	1.977±0.016
	48	6±1	27±2	30±3	12±1	25±1	2.125±0.012
	49	16±1	24±1	25±2	11±1	24±1	2.069±0.025
	50	5±1	25±1	28±2	17±1	25±1	2.042±0.006
	51	12±2	24±1	25±2	17±1	22±1	2.024±0.013
Doped with Sm & Y	52	6±1	13±1	29±2	28±1	24±1	1.923±0.021
	53	6±1	17±1	27±2	27±1	23±1	1.987±0.026
	54	13±1	6±1	30±2	27±1	24±1	2.012±0.023
	55	12±2	17±1	25±1	24±1	22±1	1.982±0.007
	56	17±2	6±1	29±3	25±1	23±1	2.002±0.011
	57	16±2	12±1	26±2	24±1	22±1	2.024±0.018
Doped with Sm & La	58	30±4	6±1	13±1	27±2	24±2	1.971±0.041
	59	26±2	6±1	18±2	26±2	24±1	1.982±0.024
	60	30±2	12±1	6±1	27±1	25±2	1.982±0.02
	61	25±2	12±1	18±2	23±1	22±1	2.002±0.007
	62	28±2	17±1	6±1	26±1	23±2	1.94±0.023
	63	23±3	17±1	13±1	24±1	23±1	2.016±0.013
Doped with La & Pr	64	28±2	27±1	7±1	27±1	11±1	2.136±0.029
	65	26±2	25±1	7±1	26±1	16±1	2.1±0.036
	66	29±1	26±1	13±1	27±1	5±1	2.223±0.004
	67	24±1	23±1	13±1	24±1	16±1	2.067±0.019
	68	26±2	25±1	18±1	26±1	5±1	2.267±0.016
	69	23±2	24±1	18±1	24±1	11±1	2.136±0.006
Doped with Pr & Sm	70	27±2	12±1	29±2	27±1	5±1	2.258±0.021
	71	27±2	17±1	26±1	25±1	5±1	2.244±0.007
	72	27±3	6±1	30±3	26±1	11±1	2.11±0.006
	73	26±3	17±1	25±3	22±1	10±1	2.164±0.028
	74	27±3	6±1	26±2	25±2	16±1	2.029±0.013
	75	25±2	11±1	25±2	24±1	15±1	2.049±0.016
Doped with Sm & Ce	76	28±1	6±1	28±1	11±1	26±1	2.01±0.015
	77	27±2	5±1	27±1	17±1	24±1	1.989±0.028
	78	27±3	12±1	29±3	7±1	25±2	2.08±0.013
	79	24±3	11±1	26±1	16±1	23±1	2.042±0.011
	80	27±4	17±1	25±3	6±1	25±2	2.106±0.03
	81	26±1	17±1	24±1	10±1	23±1	2.068±0.003

Doped with Ce & Pr	82	27±3	26±2	30±3	6±1	11±1	2.165±0.036		
	83	27±1	26±2	25±2	6±1	16±1	2.149±0.043		
	84	28±1	27±1	28±2	12±1	5±1	2.206±0.031		
	85	26±4	22±2	26±3	11±1	15±1	2.066±0.009		
	86	26±1	26±1	26±1	17±1	5±1	2.245±0.005		
	87	24±2	23±2	27±2	16±2	10±1	2.148±0.008		
Doped with Pr & Y	88	12±1	26±2	29±2	27±1	6±1	2.243±0.014		
	89	16±2	25±1	28±2	26±1	5±1	2.259±0.014		
	90	6±1	27±1	28±2	28±2	11±1	2.077±0.017		
	91	15±2	23±2	26±3	25±1	11±1	2.155±0.012		
	92	5±1	24±1	30±2	25±1	16±1	2.073±0.006		
	93	11±1	23±1	26±1	24±1	16±1	2.08±0.01		
Doped with Y & La	94	6±1	27±1	13±2	28±1	26±1	1.97±0.02		
	95	7±1	26±2	18±1	25±1	24±1	1.968±0.022		
	96	11±1	28±2	7±1	28±1	26±1	1.94±0.038		
	97	12±1	23±1	18±1	25±1	22±1	1.942±0.016		
	98	17±2	25±1	7±1	26±1	25±2	1.995±0.011		
	99	17±1	24±1	13±1	24±1	22±1	1.986±0.014		
Doped with La & Ce	100	26±3	26±1	7±1	11±1	30±3	1.974±0.013		
	101	26±3	25±2	6±1	18±2	25±2	2.055±0.041		
	102	29±2	27±1	13±1	6±1	25±1	2.079±0.024		
	103	26±3	24±1	11±1	16±1	23±1	2.043±0.016		
	104	28±3	25±1	17±2	6±1	24±1	2.007±0.015		
	105	26±1	24±1	17±1	10±1	23±1	2.06±0.017		
HEO	106	19±3	19±1	22±2	21±2	19±1	2.069±0.026	2.06[29]	[29]

9. References

[1] A. Sarkar, R. Djenadic, N. J. Usharani, K. P. Sanghvi, V. S. K. Chakravadhanula, A. S. Gandhi, H. Hahn, S. S. Bhattacharya, *J. Eur. Ceram. Soc.* **2017**, *37*, 747.

[2] M. Mishra, P. Kuppusami, T. N. Sairam, A. Singh, E. Mohandas, *Appl. Surf. Sci.* **2011**, *257*, 7665.

[3] G. Y. Adachi, N. Imanaka, *Chem. Rev.* **1998**, *98*, 1479.

[4] M. G. Paton, E. N. Maslen, *Acta Crystallogr.* **1965**, *19*, 307.

[5] O. V. Chudinovych, S. F. Korichev, E. R. Andrievskaya, *Powder Metall. Met. Ceram.* **2020**, *58*, 599.

[6] H. Kohlmann, *Zeitschrift fur Naturforsch. - Sect. B J. Chem. Sci.* **2019**, *74*, 433.

[7] A. V. Prokofiev, A. I. Shelykh, B. T. Melekh, *J. Alloys Compd.* **1996**, *242*, 41.

[8] H. Müller-Buschbaum, H. G. V. Schnering, *ZAAC - J. Inorg. Gen. Chem.* **1965**, *340*, 232.

[9] M. Yashima, S. Kobayashi, *Appl. Phys. Lett.* **2004**, *84*, 526.

[10] H. J. Osten, E. Bugiel, J. Dabrowski, A. Fissel, T. Guminskaya, J. P. Liu, H. J. Müssig, P. Zaumseil, in *Ext. Abstr. Int. Work. Gate Insul. IWGI 2001*, Institute Of Electrical And Electronics Engineers Inc., **2001**, pp. 100–106.

[11] H. J. Osten, J. P. Liu, H. J. Müssig, *Appl. Phys. Lett.* **2002**, *80*, 297.

[12] S. Kern, C. K. Loong, J. Faber, G. H. Lander, *Solid State Commun.* **1984**, *49*, 295.

[13] R. Srinivasan, R. Yogamalar, A. Vinu, K. Ariga, A. C. Bose, *J. Nanosci. Nanotechnol.* **2009**, *9*, 6747.

[14] M. Mitric, J. Blanusa, T. Barudzija, Z. Jaglicic, V. Kusigerski, V. Spasojevic, *J. Alloys Compd.* **2009**, *485*, 473.

[15] R. C. Deus, J. A. Cortés, M. A. Ramirez, M. A. Ponce, J. Andres, L. S. R. Rocha, E. Longo, A. Z. Simões, *Mater. Res. Bull.* **2015**, *70*, 416.

[16] X. Cao, R. Vassen, W. Fischer, F. Tietz, W. Jungen, D. Stöver, *Adv. Mater.* **2003**, *15*, 1438.

[17] V. Besikiotis, C. S. Knee, I. Ahmed, R. Haugsrud, T. Norby, *Solid State Ionics* **2012**, *228*, 1.

[18] A. C. Cabral, L. S. Cavalcante, R. C. Deus, E. Longo, A. Z. Simões, F. Moura, *Ceram. Int.* **2014**, *40*, 4445.

[19] R. Chiba, H. Taguchi, T. Komatsu, H. Orui, K. Nozawa, H. Arai, *Solid State Ionics* **2011**, *197*, 42.

[20] L. H. Reddy, G. K. Reddy, D. Devaiah, B. M. Reddy, *Appl. Catal. A Gen.* **2012**, *445–446*, 297.

[21] V. Vibhu, A. Flura, A. Rougier, C. Nicollet, S. Fourcade, T. Hungria, J. C. Grenier, J. M. Bassat, *J. Energy Chem.* **2020**, *46*, 62.

[22] Y. Zhao, K. Kita, K. Kyuno, A. Toriumi, *Appl. Phys. Lett.* **2009**, *94*, 042901.

[23] M. Bharathy, A. H. Fox, S. J. Mugavero, H. C. zur Loye, *Solid State Sci.* **2009**, *11*, 651.

[24] J. A. Lussier, K. M. Szkop, A. Z. Sharma, C. R. Wiebe, M. Bieringer, *Inorg. Chem.* **2016**, *55*, 2381.

[25] M. S. Anwar, S. Kumar, N. Arshi, F. Ahmed, Y. J. Seo, C. G. Lee, B. H. Koo, *J. Alloys Compd.* **2011**, *509*, 4525.

[26] H. Wu, X. Lei, J. Zhang, J. Yu, S. Zhang, *Mater. Res. Bull.* **2014**, *57*, 320.

[27] V. Sarasamma Vishnu, M. Lakshmipathi Reddy, *Sol. Energy Mater. Sol. Cells* **2011**, *95*, 2685.

[28] G. Brauer, H. Gradinger, *ZAAC - J. Inorg. Gen. Chem.* **1954**, *276*, 209.

[29] A. Sarkar, C. Loho, L. Velasco, T. Thomas, S. S. Bhattacharya, H. Hahn, R. R. Djenadic, *Dalt. Trans.* **2017**, *46*, 12167.

[30] A. I. Ivanov, I. I. Zver'kova, E. V. Tsipis, S. I. Bredikhin, V. V. Kharton, *Russ. J. Electrochem.* **2020**, *56*, 139.

[31] M. Basavad, H. Shokrollahi, H. Ahmadvand, S. M. Arab, *Ceram. Int.* **2020**, *46*, 12015.

[32] Q. H. Yang, H. X. Zhou, S. Z. Lu, *Chinese Phys. B* **2010**, *19*, 020701.

[33] N. Poovarawan, K. Suriye, J. Panpranot, W. Limsangkass, A. Guntida, F. J. C. S. Aires, P. Praserthdam, *Catal. Today* **2018**, *309*, 43.

[34] M. AKINC, D. SORDELET, *Adv. Ceram. Mater.* **1987**, *2*, 232.

[35] B. Li, H. J. Zhang, Q. Yang, Z. Bian, J. Xu, in *Opt. InfoBase Conf. Pap.*, **2009**, p. TUP6_19.

10. Chemical Composition, X-ray diffractogram, Raman spectra, and UV-vis spectra for all the 106 samples.